Impact of low NO$_x$ strategies on holistic emission reduction from a CI engine over transient conditions

Adriaan van Niekerk, **Benjamin Drew**, **Neil Larsen** and **Peter Kay**

Abstract

The use of biofuels to replace fossil fuels as well as more stringent emission regulations for internal combustion engines cause a challenge for the engine manufacturers to build engines that can cope with a wide range of fuels, but still offer low exhaust emissions with no detriment to performance. In this work a test bed with a compression ignition engine has been used to measure emissions when using a ternary fuel blend between diesel, biodiesel and ethanol together with exhuast gas recirculation (EGR) and different fuel delivery techniques. EGR with biofuels have the potential to significantly reduce NO$_x$ over conventional diesel combustion. The fuel used, B2E9 achieves a 10% renewable content as set out in the UK government's Renewable Energy Directive. Most studies reported in the literature evaluates emissions reduction technologies by only changing *one factor-at-a-time* at steady state conditions. This paper addresses these issues and presents a methodology utilising a Central Composite Design (CCD) analysis to optimise four engine parameters which include EGR percentage, main injection SOI, pilot injection SOI and pilot injection open duration over a transient drive cycle (WLTP) which makes the results more applicable to real world driving conditions. The optimisation of the CCD showed that NO$_x$ emissions decreases by 25% when the maximum exhaust gas recirculation is set to 45%, the main injection is retarded by 2 CADs, the pilot injection dwell time is set to 21 CADs and 24% of the fuel is delivered through the pilot injection. CO emissions increase by approximately 47% as a result of the decrease in NO$_x$ emissions.

Introduction

The European Union (EU) has implemented emission standards to reduce the environmental impact of road transport. These measures include the Euro 6 legislation, which enforces limitations on harmful gasses in vehicle exhaust. Viable after-treatment systems are available to meet the new emission limits, but higher costs, durability issues, fuel economy penalties and ever-increasing space requirements limit the widespread adoption of the devices. As a result, improvements to in-cylinder strategies to further reduce the engine-out emissions to decrease the burden put on after-treatment systems, are of great interest.[1] Lowering NO$_x$ emissions with exhaust gas recirculation (EGR) is a promising combustion concept that can result in the significant reduction in after-treatment dependencies.[2] Exhaust gas recirculation (EGR) dilutes the combustion materials in the cylinder by either ensuring the mixture is lean or that there is a moderate level of exhaust gas present. The exhaust gas increases the heat capacity of the combustion mixture, thus reducing the combustion temperature.[3,4] The application of EGR (usually $<50\%$) reduces the volumetric efficiency of the engine due to the rise in inlet charge temperature with less dense, hot exhaust gas replacing cool inlet air. The oxygen content of the combustion mixture is also reduced when using EGR. As a result, the local flame temperature during combustion is reduced, which reduces the formation of NO$_x$ gasses.[3,5] Unburned hydrocarbons (UHC) and CO emissions also increase with increasing use of

University of the West of England, Bristol, UK

Corresponding author:
Adriaan van Niekerk, University of the West of England, Coldharbour Lane, Bristol BS16 1QY, UK.
Email: adriaan.vanniekerk@uwe.ac.uk

EGR. To try and reduce HC, CO and PM/PN emissions, increasing the fraction of the combustion mixture that burns in the premixed phase can decrease these emissions. For blends with high oxygen content, Huang et al.[6] found that the high volatility and low cetane number enhances the mixing of the air and fuel which results in a more homogeneous mixture, which promotes complete combustion as the presence of oxygen can promote the particle oxidation process. Also, longer ignition delay periods and larger proportions of premixed combustion can be a reason for lower PM emissions of higher alcohol fuel blends. Soot forms in the fuel-rich areas of the combustion zone and by increasing the premixed burn fraction, can reduce or eliminate fuel-rich zones. Multiple fuel injections can also be used to achieve an increase in the premixed combustion fraction. Plamondon and Seers[7] found that while the addition of 20% waste cooking oil biodiesel to a binary blend increased PM emissions and decreased NO_x emissions with respect to diesel, a pilot and main injection strategy decreased both pollutants below the level observed with a single injection. Most engines currently incorporate the pilot main (P-M) injection strategy. Biswas et al.[8] investigated the use of different multiple injection scenarios which include pilot, main and after injections (P-M-A) and early, pilot, main and after injections (E-P-M-A). The results show that adding an early injection to a P-M-A strategy lowers the NO_x, CO and THC emissions, while keeping PM emissions the same. The early injection promotes the mixture of the fuel with the air in the cylinder and as the piston reaches top dead centre (TDC) it creates an almost homogeneous environment. Carlucci et al.[9] found that the duration and timing of injections such as the pilot injection have an effect on the formation of NO_x and PM emissions. By advancing the pilot injection timing, PM emissions can be reduced, as the pilot injection increases the main injection delay which results in the reduction of diffusive combustion. Zhang et al.[10] also reported a reduction in CO and PM emissions by advancing the pilot injection. The pilot injection duration was shown to have a major effect on the formation of NO_x. By increasing the injection duration, cylinder temperatures will increase, resulting in an increase in NO_x emissions. The increased duration of the pilot injection also decreases the main injection delay, which reduces NO_x formation. Mathivanan et al.[11] compared combustion of diesel using only a main injection with the emissions from combusting diesel using multiple injections. Multiple injections reduced the engine out NO_x emissions from approximately 381 ppm to 17 ppm. Mathivanan et al.[11] also reported that decreasing the duration of the pilot injection will result in the retarded combustion of the main injection, which decreases the formation of NO_x gasses. The use of multiple injections such as the E-P-M injection strategy can ultimately reduce both PM emissions and NO_x emissions.

Table 1. Effect of different strategies on combustion temperature and air-fuel mixture.[12]

Strategy	Combustion temperature	Charge homogeneity
Increase pilot injection duration	+	+
Advance pilot injection SOI	+	+
Advance main injection SOI	+	−
Increase EGR percentage	−	+

For the purposes of this research, the change of different engine operating parameters will be categorised into two groups, parameters that can reduce combustion temperature and parameters that can increases the homogeneity of the air-fuel mixture. Table 1 summarises the effects that the change of the engine parameters have on combustion temperature and charge homogeneity. The + sign indicates an increase in value and the − sign indicates a decrease in value. The change in these engine operating parameters has contrasting effects on cylinder temperature and air-fuel mixture. This research aims to optimise the different engine operating parameters identified in Table 1 to ensure their opposing and complimentary effects on the combustion temperature and charge homogeneity result in emissions reduction.

DoE allows for the investigation of multiple factors and their effect on engine emissions. The levels of the factors are changed simultaneously, rather than one at a time. This contributes to a cost and time saving.[13,14] The use of DoE is appropriate as other studies have used it successfully to investigate the effects between injection timing, injection pressure and nozzle tip protrusion on emission characteristics,[15] to analyse the role of the injection system parameters on engine emissions, noise and fuel consumption[16] and to determine the optimum composition of a ternary fuel blend that will reduces emissions when tested over the WLTP.[17]

The use of biofuels together with EGR can also be beneficial in reducing engine emissions further.[18] He et al.[19] and Huang et al.[6] concluded that adding alcohols to the fuel blend dilutes the aromatics content of the fuel which tends to decrease the soot precursors. Although using biodiesel and ethanol increases the NO_x emissions due to higher in-cylinder temperatures, this can be mitigated using EGR. Mofijur et al.[20] reviewed the available literature and suggested that the NO_x emissions can be countered with the use of exhaust gas recirculation.[3,5,21] Zhang et al.[10] reported that even though high percentages of EGR can inhibit mixing between air and fuel, thus increasing PM and CO emissions even more,[22] the oxygen content of biodiesel and ethanol permits increased use of EGR, resulting in less PM and CO emissions than that of petroleum diesel. Zheng et al.[3] also showed that high percentages of EGR together with neat biodiesel can result in a decrease in NO_x emissions as well as soot
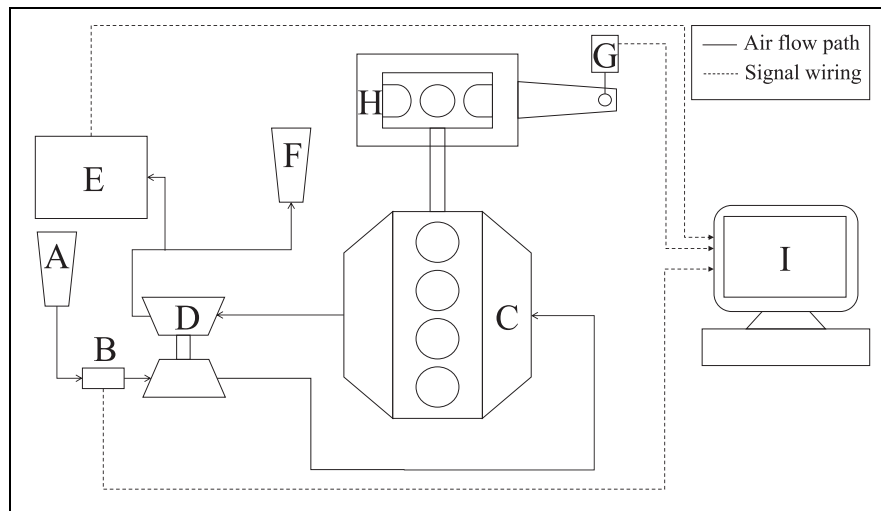
Figure 1. Layout of the engine test cell together with measuring equipment; A: air filter; B: Mass airflow sensor; C: engine; D: Turbo charger; E: gas analyser; F: exhaust outlet; G: load cell; H: dynamometer; I: DAQ.

Table 2. Physiochemical properties of B2E9.

Fuel property	Value
Cetane number	51.7
LHV (MJ/kg)	42.8
Density at 15°C (kg/m^3)	831.1
Viscosity at 40°C (mm^3/s)	2.686

Table 3. Engine parameters used for experimentation.

Engine parameter	Characteristics
Engine code	H9FB (Ford Transit)
Rated power (kW)	103
Rated torque (Nm)	375
Bore (mm)	89.9
Stroke (mm)	94.6
Volume (cm^3)	2402
Compression ratio (CR)	17.5
Number of cylinders	4
Method of cooling	Water cooled (21°C, $\sigma = 3$)

emissions. High percentages of EGR are able to counter the negative effect that neat biodiesel has on NO_x emissions. Mofijur et al.[20] also found that EGR can reduce the NO_x emissions when using biodiesel blends while still getting a reduction in CO, PM and HC emissions.

This research will use a ternary blend B2E9, which achieves the required renewable content target as set out by the European Union.[23] By using a statistical tool such as the Central Composite Design DoE during transient engine test conditions, this research will demonstrate the ability to significantly reduce in-cylinder NO_x emissions with the use of renewable fuel and optimised emission reduction strategies.

Materials and methods

The following subsections explore the set-up of the experimental equipment as well as of the Response Surface Method (RSM). The physiochemical properties provided by the fuel supplier of B2E9, are listed in Table 2.

Experimental set-up

A 2.4 L Euro IV compression ignition (CI) engine with a programmable after-market ECU was used as the test engine to collect the data. Figure 1 shows a schematic of the CI engine testing facility that was used for studying the engine emissions. The engine, with specifications listed in Table 3, was connected to a Froude FO271 dynamometer which is capable to absorbing a maximum of a 1000 kW and 4000 Nm. Three exhaust gas analysers were used; one (NOVA 7466K) for measuring NO_x emissions, (TESTO 350) for measuring CO emissions and a Pegasor M-sensor for measuring the PM and PN emissions. The use of different gas analysers ensured the highest accuracy in the measurement, as the NOVA and TESTO gas analysers have different accuracy levels for different exhaust gasses. All the gas analysers were located upstream of any exhaust after treatment systems. A summary of the analysers is presented in Table 4. The factory fitted mass airflow sensor (part number 6C11-12B579-AA), calibrated with a Superflow SF-120 flow bench, was used to measure the intake mass air flow in kg/s. Data such as engine speed, throttle position, cooling water temperature and oil sump temperature were recorded from the ECU as well as from the dynamometer control system.

Experimental design

Four engine operating variables were considered for this study. They include EGR percentage, main injection start of injection (SOI), pilot injection SOI and pilot injection duration. The engine responses include
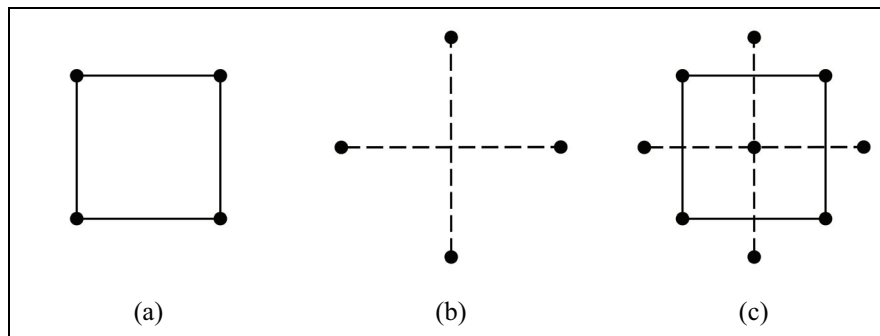
Figure 2. Central composite design.[14] (a) Factorial experimental points. Factors on the cube corners are coded -1 and $+1$. (b) Axial points of the design situated α away from design center point. (c) Factorial and axial points together with center point. Design center point is at (0,0).

Table 4. Method and accuracy of the instruments used to measure the engine emissions.

Exhaust gas	Range	Accuracy	Method
CO (ppm)	$0 - 10,000$	< 10	Electrochemical
CO_2 (%)	$0 - 20$	< 0.2	Infra-red
NO (ppm)	$0 - 2000$	< 20	Electrochemical
NO_2 (ppm)	$0 - 800$	< 8	Electrochemical

Table 5. Independent variables and their levels for a central composite design RSM.

Independent variable	Variable levels				
	-2	-1	0	1	2
EGR (%)	0	12.5	25	37.5	50
θ_{minj}– Main SOI offset (CAD)	-6	-3	0	3	6
θ_{pinj}– Pilot SOI offset (CAD)	5	9	13	17	21
$\Delta\theta_{pinj}$– Pilot duration (%)	5	16	27	38	49

CO emissions, CO_2 emissions, NO_x emissions and particulate mass (PM) and particulate number (PN). A 2^4 central composite design (CCD) was employed for the present study to obtain the experimental data, which will fit full second-order polynomial models representing the response surfaces. Figure 2 shows a schematic of what a CCD is composed of. The total number of experimental points in a CCD was calculated by the following equation:

$$N = 2^k + 2k + n_0 \tag{1}$$

where N is the number of experimental runs, k is the number of independent variables, and n_0 is the number of central points. In equation (1), 2^k is known as the factorial experimental points, $2k$ as axial points and n_0 as replicates of the center point. Factorial experimental points allow clear estimates of all main effects and interaction effects. The axial points allow the estimation of the pure quadratic effects. Centre points are designed to be run together with both the factorial points and the axial points and their replication enable the estimation of the experimental error of the RSM. For this RSM, $k = 4$ and will consist of sixteen factorial points, eighth axial points and 6 central points. A total of 30 runs will be used to analyse the data acquired from the experimental runs.

The minimum and maximum ranges of independent variables were considered and the full experimental plan with their values in un-coded and coded forms is listed in Table 5. The values for the EGR percentages shown in Table 5 indicate the maximum EGR percentage of the operating map. Examples of EGR maps that were generated for 12.5% and 50% EGR percentages can be seen in Figures 3 and 4, respectively. The maximum operating point of 50% was chosen as that was the maximum amount of EGR employed by the engine's ECU before testing started. Other published literature also investigated values of EGR in the region of 50%.[3,4,24] Zheng et al.[3] found that increasing the EGR percentage above 65% for steady-state tests on a single cylinder engine, results in cycle-to-cycle variability. Asad and Zheng[4] also concluded that the use of high percentages of EGR and high boost pressures are challenging. Engines with conventional turbochargers struggle to produce high boost and high EGR at the same time, especially at low loads. Higher boost levels require more of the exhaust to be diverted to the turbine. However, higher EGR percentages require more of the exhaust gases to be re-introduced into the intake manifold. As such, low diesel exhaust temperature at low loads places limits on the practically achievable boost pressure. Also, by investigating higher values of EGR would influence the operation of the turbocharger and ultimately influence the repeatability of the tests on the engine test cell. The limitation of the maximum EGR percentage to 50% and using the layout of the default ECU map for the EGR operation is thus acceptable.

The current ECU map for the main injection start of injection (SOI) will be used to investigate the effect of changing the SOI of the main injection. The ECU map can be seen in Figure 5. The main injection SOI map
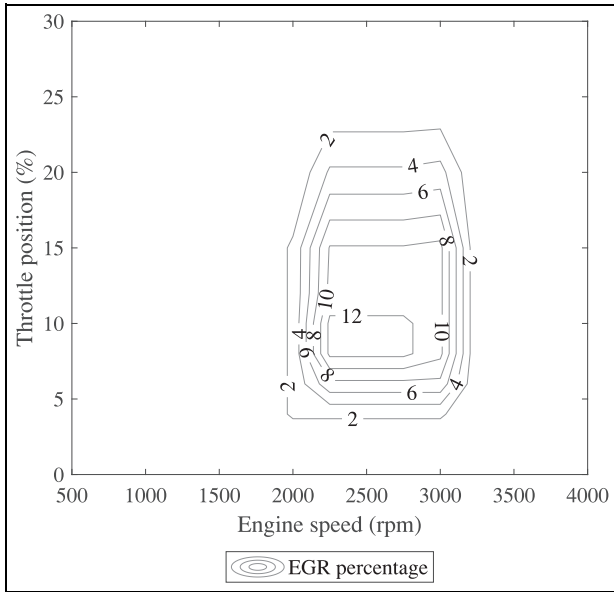
Figure 3. ECU map for a maximum EGR percentage of 12.5%.

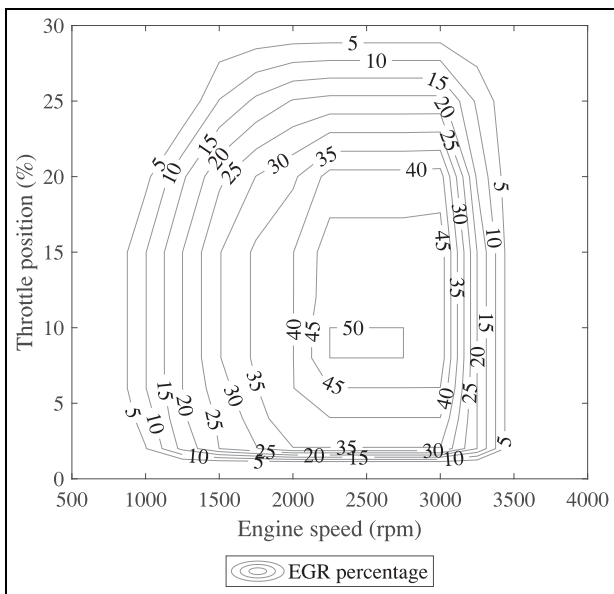**Figure 5.** Baseline ECU map for the main injection SOI.

Figure 4. ECU map for a maximum EGR percentage of 50%.

shown in Figure 5 will be changed according to the values shown in Table 5. By adding values to the main injection SOI map, the main injection SOI will become more advanced and by subtracting values from the map, the main injection SOI will become more retarded.

The operating map that will be used for the pilot injection SOI will be generated using the main injection SOI and offsetting it with the values indicated in Table 5. This can be calculated with the following equation:

$$\theta_{pinj} = \theta_{minj} + offset \tag{2}$$

where θ_{minj} and θ_{pinj} are the main injection and pilot injection SOI. The bigger the offset, the earlier the pilot
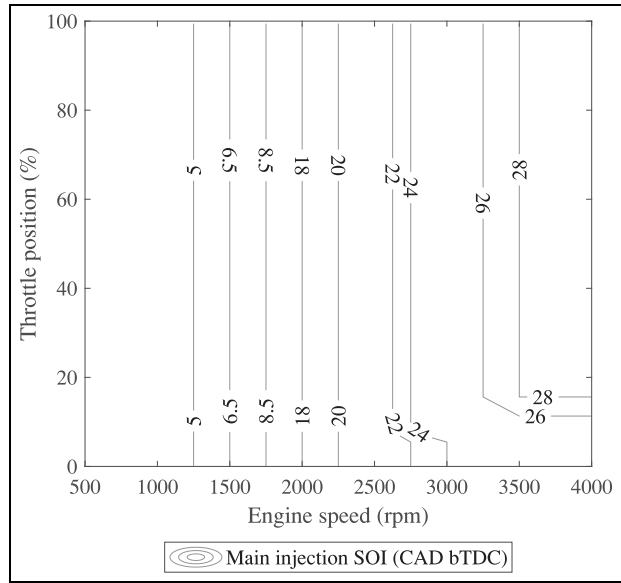
injection SOI is compared to the main injection SOI. This method of determining the pilot injection SOI was taken from published work by Beatrice et al.[25] and Biswas et al.[8] By using an offset value, it is possible to investigate the effect of dwell time of the fuel delivered through the pilot injection on emissions. Other research done by Carlucci et al.[9] and Zhang et al.[10] investigated the pilot injection SOI relative to top dead center (TDC). This method will not be effective in determining the effect of the dwell time of the fuel delivered through the pilot injection, as the main injection SOI is also changing and an advanced pilot injection relative to TDC can still have a small dwell time due to an advanced main injection. The method of offsetting the pilot injection SOI relative to the main injection SOI is thus acceptable.

The pilot duration in Table 5 is shown as a percentage of the total fuel being delivered to the engine. As the percentage of fuel introduced with the pilot injection increases, the fuel delivered through the main injection decreases accordingly. This is to ensure that the total amount of fuel entering the cylinders stay the same. The total injector open time for the whole operating envelope of the engine as a function of throttle position and engine speed was determined by adding the default ECU maps for the main injection duration and the pilot injection duration together. The summation is shown in Figure 6. The pilot injection duration (in μs) is calculated from the the map shown in Figure 6 with the following equation:

$$\Delta\theta_{pinj} = x_{pinj}\Delta\theta_{total} \tag{3}$$

where $\Delta\theta_{total}$ is the total injection duration (in μs) and x_{pinj} is the percentage of the fuel delivered through the pilot injection as shown in Table 5. The main injection duration (in μs) can thus be calculated by:
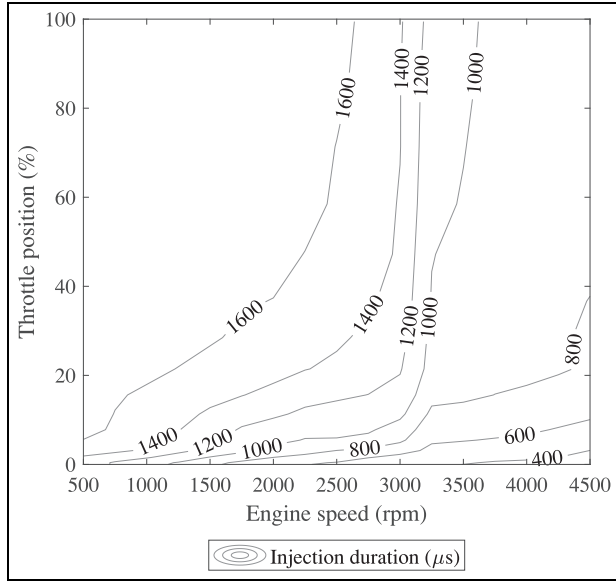
Figure 6. Total fuel delivered to the engine.

$$\Delta\theta_{minj} = \Delta\theta_{total} - \Delta\theta_{pinj} \qquad (4)$$

Expressing the fuel amount as a percentage of the total fuel delivered has been done in other research as well[10,26,27] where multiple injections were tested and the amount of fuel delivered by each injection was expressed as a percentage of the total fuel. A visual representation of the parameters used in the central composite design can be seen in Figure 7.

Optimisation of DoE

The optimisation of the engine operating parameters is dependent on more than one engine response which include CO emissions, NO_x emissions and PN/PM emissions. The desirability approach was used for the optimisation of the engine operating parameters (EGR, θ_{minj}, θ_{pinj} and $\Delta\theta_{pinj}$) for the emissions of the engine mentioned. The software transforms each response to a dimensionless desirability value d. The value ranges from $d = 0$, which indicates that the response is unacceptable, to $d = 1$ which shows that the response is more desirable. The goal of this study was to minimise all engine emissions and the desirability of each of the responses was calculated using[28]:

$$d_i(\hat{Y}_i) = \begin{cases} 1 & \text{if } \hat{Y}_i(x) < T_i \\ \frac{\hat{Y}_i(x) - U_i}{T_i - U_i} & \text{if } T_i \leqslant \hat{Y}_i(x) \leqslant U_i \\ 0 & \text{if } \hat{Y}_i \geqslant U_i \end{cases} \qquad (5)$$

where $d_i(\hat{Y}_i)$ is the desirability function of response $\hat{Y}_i(x)$, T_i and U_i are the target and upper values respectively that are desired for response $\hat{Y}_i(x)$. For minimising the response, T_i will denote a small enough value for the response. The individual desirability functions are combined using the geometric mean, which gives the overall desirability:

$$D = (d_1(Y_1)d_2(Y_2))^{0.5} \qquad (6)$$

It is noticeable that if any response $d_i(\hat{Y}_i)$ is completely undesirable, $d_i(\hat{Y}_i) = 0$, then the overall desirability is zero.

Data collection

The engine was run on the WLTP as shown in Figure 8. The WLTP shows the variation of vehicle speed with time. Since only the engine and not the whole vehicle was tested it is necessary to relate the vehicle speed to the engine speed and load, based on the vehicle characteristics such as gear ratio etc. The method used is presented elsewhere.[29]
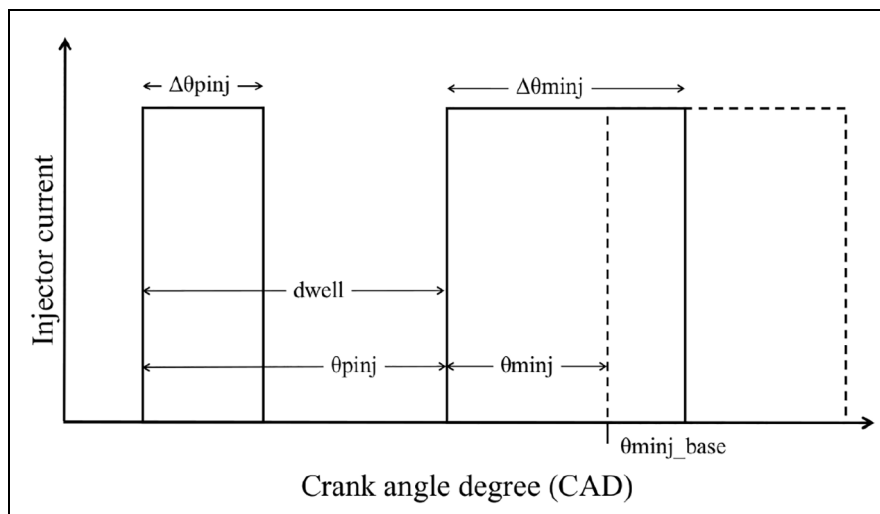

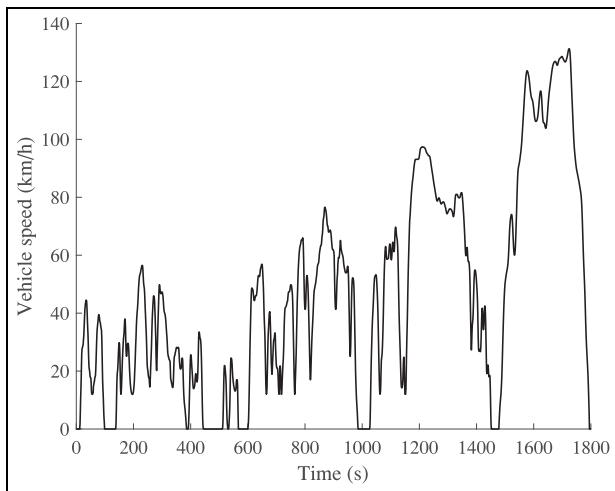**Figure 7.** Visual representation of the parameters listed in Table 5.

Figure 8. The World Harmonised Light Vehicle Test Procedure used in the type approval of new vehicles as per EU regulation 2017/1151.[30]

Results

In this section, the effects of changing different engine operating parameters on different engine responses were considered. These engine operating parameters include exhaust gas recirculation (EGR) percentage, main injection SOI (θ_{minj}), pilot injection SOI (θ_{pinj}) and pilot injection duration ($\Delta\theta_{pinj}$). Engine emissions were investigated over the WLTP drive cycle. Table 6 shows the engine emission results for the different DoE tests. Test 25 and test 26 could not be completed as the combination of the engine parameters prevented the engine from following the drive cycle accurately. Table 7 shows the p-values of each engine parameter that was varied in the RSM. The principal model analysis was based on the analysis of variance (ANOVA) which provided statistical information including the p-values of the different model terms. p-values of less than 0.02 are deemed as highly significant, which means that the probability of this phenomena is due to chance, is less than 2%.[31,32] Engine parameters that have a significant effect on the engine emissions over the WLTP drive cycle will the discussed in detail. The use of graphs illustrating the main effect plots as well as the interaction plots between different engine parameters will also be illustrated. The higher the gradient of the line plots, the more significant effect the engine parameter has on the engine emissions response. Where possible, emissions over time for different DoE tests are compared and discussed.

CO emissions

The quadratic model developed for the CO emissions as fitted based on the RSM design corresponds to:

$$Z_{CO} = 2.01 - 0.0088 \times EGR - 0.035 \times \theta_{pinj}$$
$$- 0.0307 \times \Delta\theta_{pinj} + 0.002126 \times \Delta\theta_{pinj} \times \Delta\theta_{pinj}$$
$$+ 0.00801 \times \theta_{minj} \times \Delta\theta_{pinj} - 0.00489 \times \theta_{pinj} \times \Delta\theta_{pinj}$$

$$(7)$$

where Z_{CO} is the CO emissions in the exhaust gas of the engine in grams per kilometer. High values of R^2 (91.31%) and adjusted R^2 (80.24%) for equation (7) indicate a high correlation between the experimental CO emissions and the RSM predicted values of the CO emissions. Figure 9 visually show the main effects and interaction effects of the engine parameters on the engine's CO emissions. For the experimental CO emissions the linear terms EGR, θ_{pinj} and $\Delta\theta_{pinj}$, the quadratic term for $\Delta\theta_{pinj}$ and the two-way interaction effects between θ_{minj} and $\Delta\theta_{pinj}$ and θ_{pinj} and $\Delta\theta_{pinj}$ are deemed significant with $p < 0.02$. The increase in EGR percentage from zero to a maximum of 50% has a negative effect on the formation of CO emissions, as seen in Figure 9(a).

Figure 9(a) shows that CO emissions decrease by increasing θ_{pinj} of the pilot injection fuel (increasing the gap between the SOI of the pilot injection and the main injection SOI). By offsetting the pilot injection SOI by approximately 18 CAD a maximum reduction of CO emissions can be achieved. Beatrice et al.[25] similarly reports that by increasing the difference between the pilot injection SOI and main injection SOI from 7 CAD to 10 CAD when running the engine at 1500 rpm and 2 BMEP load, the CO emissions reduced from 800 ppm to 600 ppm. The increased dwell time promotes the stratification of the fuel in the cylinder and as the cylinder piston reaches top dead centre (TDC) it creates an almost homogeneous environment, which enables the increased oxygenation of CO gasses. Figure 10 shows a time series plot for CO emissions of test 8 and test 15, which have different pilot injection offsets (θ_{pinj}) with the WLTP drive cycle shown in dashed lines. The differences in CO emissions between the two tests considered in Figure 10 are minor except at idling scenarios in the WLTP. CO emissions are at its highest during idling, as the fuel and air does not mix properly to ensure improved combustion. By increasing the offset of the pilot injection SOI compared to the main injection SOI, fuel has more time to mix with the air and improve overall combustion. This can be seen in Figure 10 where CO emissions are reduced during idling (0 km/h) for a pilot injection offset of $\theta_{pinj} = 17$ CAD.

The percentage fuel delivered through the pilot injection also significantly influences the formation of CO emissions. Engine CO emissions can be kept to a minimum if approximately 20% of the total fuel is delivered through the pilot injection. The increase in fuel delivered through the pilot injection, increases the amount of fuel available to mix with the intake air, before combustion occurs and thus increases the fraction of fuel burned in the premixed combustion phase. Figure 9(a) also shows that by increasing the amount of fuel delivered by the pilot injection past 20%, increases the CO emissions generated by the engine. Carlucci et al.[9] reported a similar phenomena where a certain percentage of the fuel delivered through the pilot injection, promoted the homogeneity of the air fuel mixture prior to combustion. For small percentages of fuel delivered

Table 6. The simulated and experimental values for the engine emissions for the RSM.

Run	Parameter settings				Experimental results			
	EGR (%)	θ_{minj}(CAD)	θ_{pinj} (CAD)	$\Delta\theta_{pinj}$ (%)	CO (g/km)	NO$_x$ (g/km)	PN (#/km)	PM (g/km)
1	12.5	3	17	38	1.9453	1.9775	1.676E + 14	0.0367
2	12.5	3	9	16	1.2426	1.3605	2.936E + 14	0.0642
3	25.0	0	13	27	1.7885	1.0494	3.288E + 14	0.0719
4	37.5	−3	9	16	2.8163	0.7504	6.243E + 14	0.1366
5	25.0	0	13	27	2.0736	0.9113	4.492E + 14	0.0983
6	12.5	3	9	38	3.1093	1.9169	3.800E + 14	0.0831
7	12.5	−3	9	38	2.2036	1.3641	3.896E + 14	0.0852
8	37.5	3	9	16	1.6643	1.0377	1.782E + 14	0.0390
9	37.5	−3	17	16	2.2079	0.8464	3.594E + 14	0.0786
10	12.5	−3	17	16	1.9418	1.0283	2.841E + 14	0.0621
11	12.5	3	17	16	1.4127	1.6963	1.512E + 14	0.0331
12	37.5	3	9	38	3.9093	1.7396	3.283E + 14	0.0718
13	12.5	−3	17	38	2.0617	1.5207	1.357E + 14	0.0297
14	37.5	3	17	38	2.6105	1.8798	8.892E + 13	0.0195
15	37.5	3	17	16	1.5471	1.2556	1.198E + 14	0.0262
16	12.5	−3	9	16	2.0409	1.0370	1.811E + 14	0.0396
17	37.5	−3	9	38	2.1625	1.0166	1.768E + 14	0.0387
18	25.0	0	13	27	1.9350	1.0658	1.250E + 14	0.0273
19	25.0	0	13	27	2.0489	1.0458	1.119E + 14	0.0245
20	37.5	−3	17	38	2.3646	1.1140	6.477E + 13	0.0142
21	25.0	0	13	27	1.6210	1.2511	4.644E + 13	0.0102
22	25.0	0	13	5	1.9477	0.9864	8.977E + 13	0.0196
23	25.0	0	13	27	1.7582	1.2017	4.066E + 13	0.0089
24	50.0	0	13	27	1.8820	1.0034	4.545E + 13	0.0099
25	25.0	0	13	49	−	−	−	−
26	25.0	0	5	27	−	−	−	−
27	25.0	−6	13	27	2.2099	1.0375	5.844E + 13	0.0128
28	25.0	0	21	27	1.7612	1.2637	3.515E + 13	0.0077
29	25.0	6	13	27	1.5436	1.4842	2.351E + 13	0.0051
30	0.0	0	13	27	1.6397	1.2513	3.799E + 13	0.0083

Table 7. p-Values for the engine response of the simulated and experimental RSM.

	Experimental results		
	CO	NO$_x$	PN/PM
Model	<0.02	<0.02	<0.02
Linear	<0.02	<0.02	0.08
EGR	<0.02	<0.02	0.20
θ_{minj}	0.23	<0.02	0.59
θ_{pinj}	<0.02	0.13	<0.02
$\Delta\theta_{pinj}$	<0.02	<0.02	0.83
Square	<0.02	<0.02	<0.02
EGR × EGR	0.65	0.64	0.47
$\theta_{minj} \times \theta_{minj}$	0.89	<0.02	0.47
$\theta_{pinj} \times \theta_{pinj}$	0.25	0.43	0.50
$\Delta\theta_{pinj} \times \Delta\theta_{pinj}$	<0.02	<0.02	<0.02
2-way interaction	<0.02	0.26	<0.02
EGR × θ_{minj}	0.62	0.21	0.68
EGR × θ_{pinj}	0.59	0.37	0.40
EGR × $\Delta\theta_{pinj}$	0.12	0.65	0.17
$\theta_{minj} \times \theta_{pinj}$	0.20	1.00	0.07
$\theta_{minj} \times \Delta\theta_{pinj}$	<0.02	<0.02	0.08
$\theta_{pinj} \times \Delta\theta_{pinj}$	<0.02	0.62	<0.02
Lack-of-fit	0.16	0.82	0.25

through the pilot injection, the mixture is too lean for autoignition to occur even with the increased pressure and temperature produced by the compression stroke of the engine. When the percentage of fuel increases past a certain point, autoignition of the fuel injected through the pilot injection can occur and this reduces the ignition delay of the main injection, due to increased temperatures and pressures. The reduced ignition delay causes the majority of the fuel delivered through the main injection to burn in the diffusion combustion phase which increases the formation of CO emissions.[3] If more than 40% of the fuel is delivered through the pilot injection, it can also start influencing the performance of the engine with an increase in incomplete combustion which also results in an increase of CO emissions.

The interaction effects between θ_{minj} and $\Delta\theta_{pinj}$ and θ_{pinj} and $\Delta\theta_{pinj}$ are shown in Figure 9(b). The interaction effects between θ_{minj} and $\Delta\theta_{pinj}$ for the experimental CO emissions show that for a $\Delta\theta_{pinj}$ of 27%, there are minor changes when changing the main injection SOI. When $\Delta\theta_{pinj}$ is 5%, CO emissions decrease when the main injection SOI is advanced. As the majority of the fuel is delivered through the main injection, by advancing the SOI of the main injection results in improved combustion as the combustion temperature is increased. When 49% of the fuel is delivered through the pilot injection, CO emissions increases when the main injection SOI is advanced. As mentioned earlier, autoignition of the fuel delivered through the pilot injection can occur when
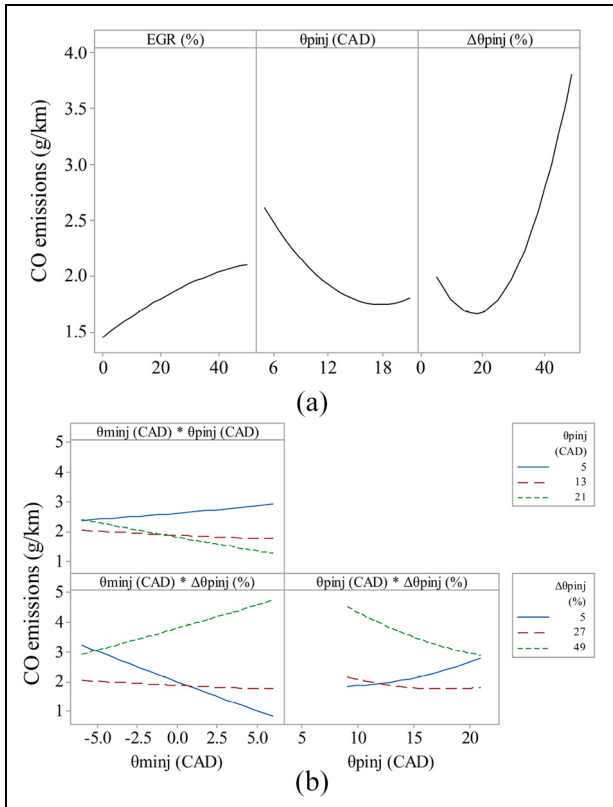
Figure 9. Response plots for the experimental CO emissions when engine operating conditions are varied. (a) Main effects plot for experimental engine CO emissions. (b) Interaction effects plot for the experimental engine CO emissions.
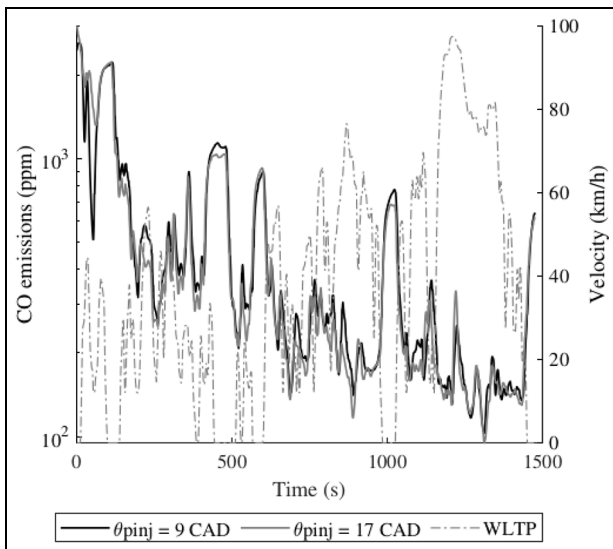

Figure 10. CO emissions comparison with θ_{pinj} at 9 CAD and 17 CAD (test 8 and 15).

higher percentages of the total fuel is delivered through the pilot injection. When advancing the main injection SOI, the ignition delay of the fuel delivered through the main injection is decreased and the majority of the fuel is burned in the diffusion combustion phase. When the main injection is retarded, the ignition delay of the main

injection is increased and more fuel is burned in the pre-mixed combustion stage, thus decreasing CO emissions.

The interaction effects between θ_{pinj} and $\Delta\theta_{pinj}$ for the experimental CO emissions show that for percentages of fuel 27% and higher, by increasing the dwell time of the pilot injection, CO emissions are decreased. About 49% fuel delivered through the pilot injection has an overall higher CO emissions result as a bigger portion of the fuel cannot mix sufficiently with the air before combustion starts, compared to when only 27% of the fuel is introduced through the pilot injection. As shown in Figure 9(b) for small percentages of fuel injected through the pilot injection, CO emissions increase when the dwell time of the pilot injection increases. As 9% of the fuel is ethanol, the high latent heat of evaporation can cool the combustion chamber down with a longer pilot injection dwell time. A cooler combustion chamber can increase the ignition delay as well and hinder complete combustion, which has a negative effect on CO emissions.

NO_x emissions

The quadratic model developed for the NO_x emissions as fitted based on the RSM design corresponds to:

$$
\begin{aligned}
Z_{NO_x} = {} & 1.614 - 0.0152 \times EGR - 0.0088 \times \theta_{minj} \\
& - 0.0227 \times \Delta\theta_{pinj} + 0.001162 \times \theta_{minj} \times \theta_{minj} \\
& + 0.000801 \times \Delta\theta_{pinj} \times \Delta\theta_{pinj} \\
& + 0.002311 \times \theta_{minj} \times \Delta\theta_{pinj}
\end{aligned}
$$

(8)

where Z_{NO_x} is the experimental NO_x emissions in the exhaust gas of the engine in grams per kilometer. High values of R^2 (95.80%) and adjusted R^2 (90.46%) respectively for equation (8) indicate a high correlation between the experimental NO_x emissions and the RSM predicted values of the NO_x emissions. Figure 11 shows the main effects and interaction effects of the four engine parameters on the engine NO_x emissions. For the NO_x emissions the linear terms EGR, θ_{minj} and $\Delta\theta_{pinj}$, the quadratic terms for θ_{minj} and $\Delta\theta_{pinj}$ and the two-way interaction effects between θ_{minj} and $\Delta\theta_{pinj}$ are deemed significant with $p < 0.02$.

When considering the effects of the changing engine parameters under investigation, NO_x emissions decrease with an increase in EGR percentage. Figure 12 shows a time series plot for NO_x emissions of test 2 and test 8, which have different EGR percentages with the WLTP drive cycle shown in dashed lines. Throughout the drive cycle, the NO_x emissions generated by the test with an EGR of 37.5% is lower than the test with an EGR of 12.5%. The difference is more pronounced at lower drive cycle speeds. The effect of EGR percentage on NO_x emissions are also deemed significant by the statistical model which is in line with the majority of research discussed.
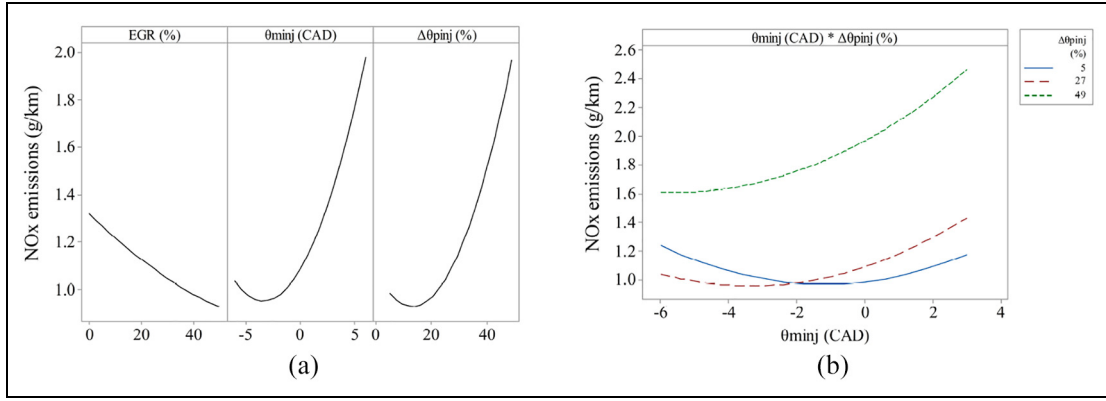
Figure 11. Response plots for experimental NO_x emissions when engine operating conditions are varied. (a) Main effects plot for the experimental engine NO_x emissions. (b) Interaction effects plot for the experimental engine NO_x emissions.

The NO_x emissions exhibit an increase when the main injection SOI is advanced and a minimum when retarding the main injection SOI map by approximately 3 CADs. Bohl et al.[33] investigated the effects of the main injection SOI on NO_x emissions when using HVO fuel and concluded that the advanced injection causes the peak pressure to be closer to TDC and therefore cylinder temperature is increased.

The increase in pilot injection duration increases the NO_x emissions. As more fuel is introduced through the pilot injection, a bigger proportion of the total fuel will burn in the premixed combustion event, thus increasing the combustion temperature as well as the NO_x emissions.

The interaction effects between θ_{minj} and $\Delta\theta_{pinj}$ can be seen in Figure 11(b). By advancing the main injection by approximately 5 CADs and delivering approximately 50% of the fuel through the pilot injection, results in the maximum amount of NO_x emissions generated. This is caused by the increase in fuel that can mix with the air before combustion occurs and with the advancement of the main injection, start of combustion occurs close to TDC, which results in higher combustion temperatures. With a decrease in the percentage of fuel delivered through the pilot injection, the NO_x emissions are reduced and the effect of changing the main injection SOI on NO_x emissions is not as pronounced.

PN/PM emissions

PN emissions and PM emissions are discussed jointly, as the voltage trap signal of the Pegasor M-sensor is converted by separate coefficients for PN and PM emissions. The quadratic models developed for the PN emissions and PM emissions as fitted based on the RSM design correspond to:

$$
\begin{aligned}
Z_{PN} = {} & 811133287725601 \\
& - 7633497409759 \times \theta_{pinj} \\
& + 1207509358289 \times \Delta\theta_{pinj} \times \Delta\theta_{pinj} \\
& - 1214678643048 \times \Delta\theta_{pinj} \times \theta_{pinj}
\end{aligned} \tag{9}
$$

and

$$
\begin{aligned}
Z_{PM} = {} & 0.1775 - 0.00167 \times \theta_{pinj} \\
& + 0.000264 \times \Delta\theta_{pinj} \times \Delta\theta_{pinj} \\
& - 0.000264 \times \Delta\theta_{pinj} \times \theta_{pinj}
\end{aligned} \tag{10}
$$

Z_{PN} and Z_{PM} are the PN emissions and PM emissions in the exhaust gas of the engine in number per kilometer and grams per kilometer. High values of R^2 (89.79%) and adjusted R^2 (73.91%) for equations (9) and (10), respectively indicate a high correlation between the experimental PN emissions and PM emissions and the RSM predicted values of the PN emissions and PM emissions. For the PN emissions and PM emissions the linear term θ_{pinj}, the quadratic terms for $\Delta\theta_{pinj}$ and the two-way interaction effects between θ_{pinj} and $\Delta\theta_{pinj}$ are deemed significant with $p < 0.02$. Figure 13(a) and (b) show that by increasing the dwell time of the pilot injection, PN emissions and PM emissions decrease. By increasing the dwell time from 5 CADs to approximately 18 CADs, PN emissions and PM emissions can be reduced by 80%. This is due to the fact that with an increased dwell time, the fuel and air mixture have longer time to mix together thoroughly. A more homogeneous mixture is formed prior to combustion, leading to a higher in-cylinder pressure and combustion temperature which promote the particle oxidation process. The interaction effects shown in Figure 13(c) and (d) also show that with a high pilot injection dwell time and injecting 49% of the fuel through the pilot injection can decrease the PN emissions and PM emissions significantly. Lower percentages ($<27\%$) result in only a limited amount of the fuel being mixed with the air and thus a bigger fraction of the fuel burns in the diffusion combustion phase. Smaller percentages of fuel injected through the pilot injection can ignite during the compression stage and decrease the ignition delay of the main injection. A shorter ignition delay for the main injection results in an increase of fuel burnt in the diffusion combustion phase which increases PN/PM emissions. Figure 13 shows that with an increase in pilot injection dwell time
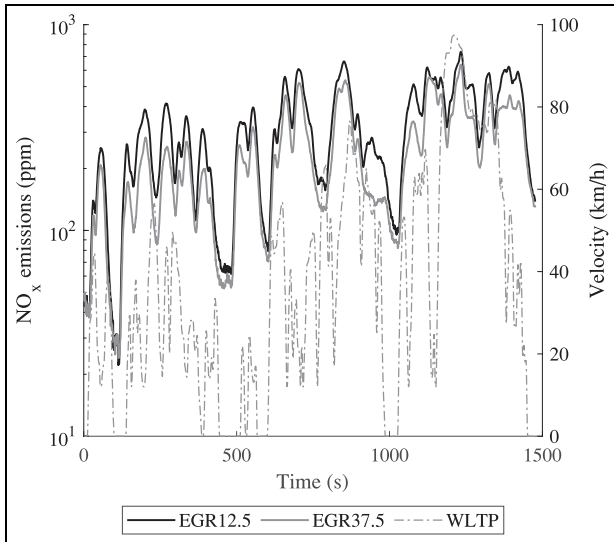
Figure 12. NO$_x$ emissions comparison with EGR at 12.5% and 37.5% (test 2 and 8).

with a small percentage of fuel injected through the pilot injection can cause a further increase in PN/PM emissions.

Optimising engine parameters

As there is more than one engine emission response to be optimised, it is necessary to set requirements for each response, that the optimisation tool will optimise towards. The desirability approach was used to minimise all engine out emissions. Figure 14 shows the desirability plot when minimising all engine emissions. The plotted lines are known as the prediction lines of the different engine emissions. The vertical solid lines for each variable is the current engine operating parameter setting. By changing the vertical solid line for each engine operating parameter, the horizontal dashed lines were updated by re-computing the predicted engine emissions for the new values of exhaust gas recirculation (EGR) percentage, main injection SOI (θ_{minj}), pilot injection SOI (θ_{pinj}) and pilot injection duration ($\Delta\theta_{pinj}$). The horizontal dashed lines show the final predicted engine emissions according to the given engine operating conditions. An overall desirability of 89% was achieved by having a maximum EGR percentage of 45%, retarding the main injection SOI map by 2 CADs, setting the offset of the pilot injection to the main injection to 21 CADs and injecting 24% of the total fuel through the pilot injection event. This will result in CO emissions of 1.92 g/km, NO$_x$ emissions of 0.80 g/km and PM emissions of 0.004 g/km. NO$_x$ emissions are reduced by 29% and CO emissions increased by 47% compared to pump diesel available at all major pumping stations.[17] The increase of EGR percentage, reduces the NO$_x$ emissions and reduces the combustion temperature. By increasing the dwell time of the pilot injection and injecting approximately 20% of the total fuel
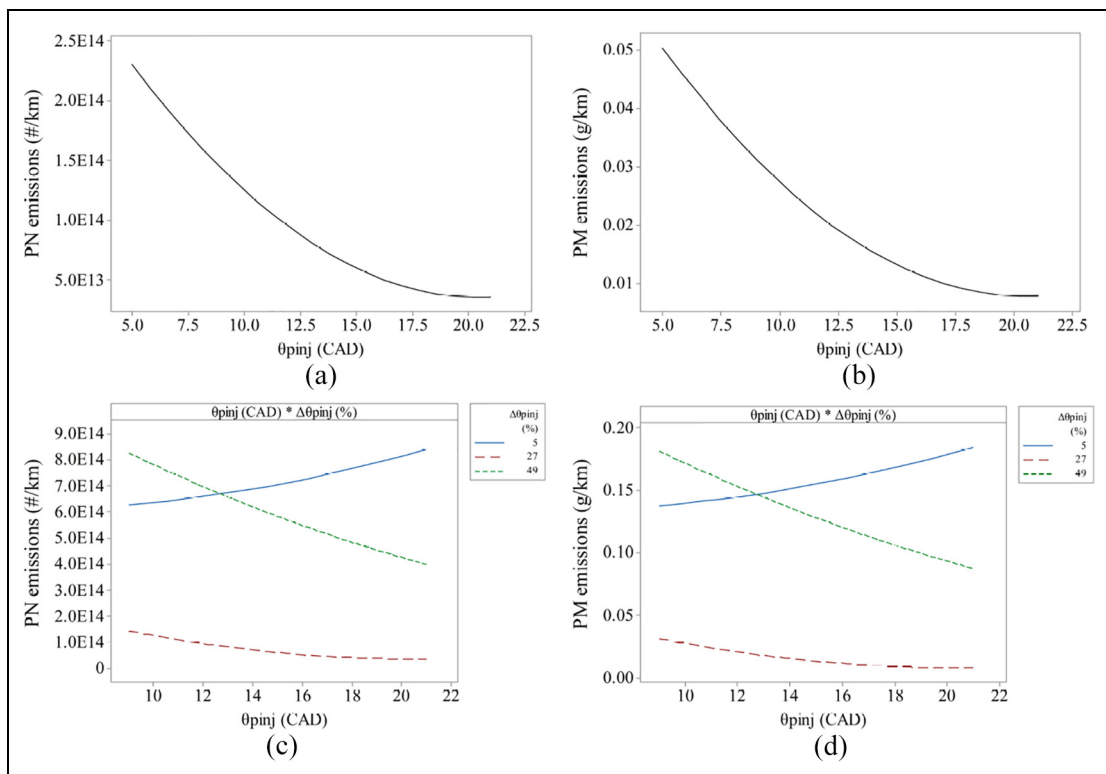

Figure 13. Main and interaction plots for PM/PN emissions when engine operating conditions are varied. (a) Main effects plot for engine PN emissions. (b) Main effects plot for engine PM emissions. (c) Interaction effects plot for engine PN emissions. (d) Interaction effects plot for engine PM emissions.
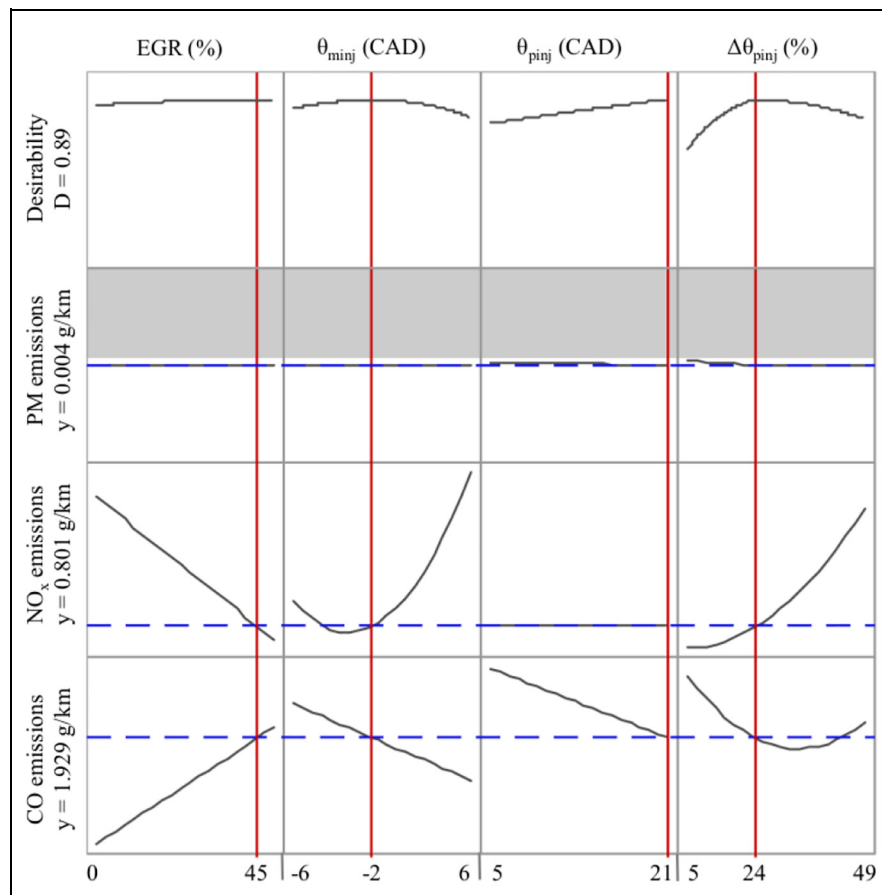
Figure 14. Optimisation plot for the engine emissions RSM.

Table 8. Summary of results showing the change in emissions compared to pump diesel.

	Pump diesel	B2E9	Optimised
CO emissions (g/km)	1.309	0.796	1.929
NOx emissions (g/km)	1.136	1.003	0.801
CO emissions	–	−34%	47%
NOx emissions	–	−10%	−29%

with the pilot injection event decreases CO emissions as a result of an increase in the homogeneity of the air fuel mixture and combustion. PM emissions are also below the legislated limit of 0.025 g/km. Table 8 shows a summary of the results and the percentage change compared to pump diesel as well as the results obtained in a previous study where only B2E9 was used.[17] NOx emissions are further reduced using an optimised fuel delivery strategy and EGR with a total reduction of 29% compared to pump diesel. CO emissions increase by 47% compared to pump diesel when the same techniques are used. The trade-off between NOx emissions and CO emissions are evident and also seen in other published work where the decrease in NOx emissions result in an increase in CO emissions.[12]

Conclusion

This study investigated the effects of engine operating parameters on the emission characteristics of a compression ignition engine fuelled with a ternary blend, B2E9. The engine was tested over the World Harmonised Light vehicle Test Procedure (WLTP). Based on a RSM DoE, 30 runs were formulated which included 6 replicates of the center point to evaluate the reproducibility and the lack-of-fit of the derived models. The main conclusions are:

1. By using a statistical tool such as the RSM DoE during transient engine test conditions, this research demonstrated the ability to significantly reduce in-cylinder NOx emissions with the use of renewable fuel and optimised emission reduction strategies.
2. NOx emissions can be reduced by approximately 29% by using a maximum of 45% EGR, retarding the main injection SOI by 2 CADs, setting the dwell time of the pilot injection to 21 CADs and injecting 24% of the total fuel through the pilot injection.
3. Even though the fuel delivery was optimised to minimise all emissions, there was still an increase

in CO emissions of approximately 47% compared to a vehicle running on pump diesel. This is due to the trade-off between NO_x emissions and CO emissions.

4. EGR can be used to reduce NO_x emissions by approximately 34% when the EGR percentage is increased from 0% to 50%. The opposite occurs for CO emissions, which increases by approximately 32% when EGR is increased to a maximum of 50%.

5. By advancing the main injection SOI, NO_x emissions increase and CO emissions decrease as a result of the start of combustion occurring closer to TDC, thus increasing the combustion temperature and combustion pressure.

6. An increase of the dwell time of the pilot injection to approximately 21 CADs can decrease CO emissions by approximately 17%, as the increased dwell time promotes the mixing of the fuel and air which causes an increase in the premixed combustion phase. A more homogeneous mixture also promotes the particle oxidation process which reduces the total PM/PN emissions.

7. By injecting more fuel through the pilot injection a higher percentage of the fuel mixes with the air before combustion commences. This increases the portion of fuel being burned in the premixed combustion phase and increases combustion temperatures. As a result NO_x emissions increase and CO emissions decrease.

8. This work demonstrated that the RSM DoE is a useful tool to quantify the effect of different engine operating parameters on the engine's emissions response. It is also useful to determine the optimum operating configuration that will meet the researcher's criteria.

Declaration of conflicting interests

The author(s) declared no potential conflicts of interest with respect to the research, authorship, and/or publication of this article.

ORCID iDs

Adriaan Smuts van Niekerk https://orcid.org/0000-0002-8010-5333
Peter John Kay https://orcid.org/0000-0002-9760-5211

References

1. Musculus MP, Miles PC and Pickett LM. Conceptual models for partially premixed low-temperature diesel combustion. *Prog Energy Combust Sci* 2013; 39(2–3): 246–283.
2. Dev S, Chaudhari HB, Gothekar S, Juttu S, Walke NH and Marathe NV. Review on advanced low temperature combustion approach for BS VI. SAE technical paper 2017-26-0042, 2017.
3. Zheng M, Mulenga MC, Reader GT, Wang M, Ting DS and Tjong J. Biodiesel engine performance and emissions in low temperature combustion. *Fuel* 2008; 87(6): 714–722.
4. Asad U and Zheng M. Efficacy of EGR and boost in single-injection enabled low temperature combustion. *SAE Int J Engines* 2009; 2(1): 1085–1097.
5. Ladommatos N, Abdelhalim S and Zhao H. The effects of exhaust gas recirculation on diesel combustion and emissions. *Int J Engine Res* 2000; 1(1): 107–126.
6. Huang H, Liu Q, Wang Q, Zhou C, Mo C and Wang X. Experimental investigation of particle emissions under different egr ratios on a diesel engine fueled by blends of diesel/gasoline/n-butanol. *Energy Convers Manag* 2016; 121: 212–223.
7. Plamondon E and Seers P. Parametric study of pilot–main injection strategies on the performance of a light-duty diesel engine fueled with diesel or a WCO biodiesel–diesel blend. *Fuel* 2019; 236: 1273–1281.
8. Biswas S, Bakshi M, Shankar G and Mukhopadhyay A. Optimization of multiple injection strategies to improve BSFC performance of a common rail direct injection diesel engine. SAE technical paper 2016-28-0002, 2016.
9. Carlucci P, Ficarella A and Laforgia D. Effects of pilot injection parameters on combustion for common rail diesel engines. SAE technical paper 2003-01-0700, 2003.
10. Zhang Q, Ogren RM and Kong SC. Trade-offs between emissions and efficiency for multiple injections of neat biodiesel in a turbocharged diesel engine using an enhanced PSO-GA optimization strategy. SAE technical paper 2016-01-0630, 2016.
11. Mathivanan K, Mallikarjuna J and Ramesh A. Influence of multiple fuel injection strategies on performance and combustion characteristics of a diesel fuelled hcci engine–an experimental investigation. *Exp Therm Fluid Sci* 2016; 77: 337–346.
12. van Niekerk AS, Kay PJ, Drew B and Larsen N. Optimisation of low temperature combustion technology, for future drive cycles, using a factorial design of experiments. SAE technical paper 2019-01-2171, 2019.
13. Minitab. Minitab 17 statistical software [computer software]. 2010, www.minitab.com (accessed 1 September 2020).
14. Montgomery DC. *Design and analysis of experiments*. Hoboken, NJ: John Wiley & Sons, 2017.
15. Pandian M, Sivapirakasam S and Udayakumar M. Investigation on the effect of injection system parameters on performance and emission characteristics of a twin cylinder compression ignition direct injection engine fuelled with pongamia biodiesel – diesel blend using response surface methodology. *Appl Energy* 2011; 88(8): 2663–2676.
16. Win Z, Gakkhar R, Jain S, et al. Investigation of diesel engine operating and injection system parameters for low noise, emissions, and fuel consumption using Taguchi

methods. *Proc IMechE, Part D: J Automobile Engineering* 2005; 219(10): 1237–1251.

17. van Niekerk AS, Drew B, Larsen N and Kay PJ. Influence of blends of diesel and renewable fuels on compression ignition engine emissions over transient engine conditions. *Appl Energy* 2019; 255.

18. Lapuerta M, Ramos A, Fernández-Rodrguez D and González-García I. High-pressure versus low-pressure exhaust gas recirculation in a Euro 6 diesel engine with lean-NOx trap: effectiveness to reduce NOx emissions. *Int J Engine Res* 2019; 20(1): 155–163.

19. He T, Chen Z, Zhu L and Zhang Q. The influence of alcohol additives and egr on the combustion and emission characteristics of diesel engine under high-load condition. *Appl Therm Eng* 2018; 140: 363–372.

20. Mofijur M, Rasul M, Hyde J, Azad AK, Mamat R and Bhuiya MM. Role of biofuel and their binary (diesel–biodiesel) and ternary (ethanol–biodiesel–diesel) blends on internal combustion engines emission reduction. *Renew Sustain Energ Rev* 2016; 53: 265–278.

21. Kumar N, Sonthalia A, Tomar M and Koul R. An experimental investigation on spray, performance and emission of hydrotreated waste cooking oil blends in an agricultural engine. *Int J Engine* Res. Epub ahead of print June 2020. DOI: 10.1177/1468087420928734.

22. Hua Y, Liu F, Wu H, et al. Effects of alcohol addition to traditional fuels on soot formation: a review. *Int J Eng Res*. Epub ahead of print April 2020. DOI: 10.1177/1468087420910886.

23. European Union. Directive 2009/28/ec of the European Parliament and of the Council of 23 April 2009 on the promotion of the use of energy from renewable sources and amending and subsequently repealing Directives 2001/77/EC and 2003/30/EC. OJ L 140, 5.6.2009, p.16–62, http://eur-lex.europa.Eu/legal-content/EN/ALL/?uri=CELEX:32009L0028&qid=1498667012776 (2009, accessed 28 June 2017).

24. Asad U, Divekar P, Zheng M and Tjong J. Low temperature combustion strategies for compression ignition engines: operability limits and challenges. SAE technical paper 2013-01-0283, 2013.

25. Beatrice C, Napolitano P and Guido C. Injection parameter optimization by DoE of a light-duty diesel engine fed by bio-ethanol/RME/diesel blend. *Appl Energy* 2014; 113: 373–384.

26. Gill K, Marriner C, Sison K and Zhao H. In-cylinder studies of multiple diesel fuel injection in a single cylinder optical engine. SAE technical paper 2005-01-0915, 2005.

27. Ehleskog R, Ochoterena RL and Andersson S. Effects of multiple injections on engine-out emission levels including particulate mass from an hsdi diesel engine. SAE technical paper 2007-01-0910, 2007.

28. NIST/SEMATECH. *e-Handbook of statistical methods.* http://www.itl.nist.gov/div898/handbook/ (2013, accessed 1 December 2017).

29. Van Niekerk AS, Kay PJ, Drew B and Larsen N. Development of multi-fidelity powertrain simulation for future legislation. In: *Internal combustion engines 2017*, Birmingham, UK, 6–7 December 2017. http://eprints.uwe.ac.uk/33589 (accessed 1 September 2020).

30. European Union. COMMISSION REGULATION (EU) 2017/1151 of 1 June 2017 supplementing Regulation (EC) No 715/2007 of the European Parliament and of the Council on type-approval of motor vehicles with respect to emissions from light passenger and commercial vehicles (Euro 5 and Euro 6) and on access to vehicle repair and maintenance information, amending Directive 2007/46/EC of the European Parliament and of the Council, Commission Regulation (EC) No 692/2008 and Commission Regulation (EU) No 1230/2012 and repealing Commission Regulation (EC) No 692/2008. OJ L 175, 7.7.2017, p.1–643. https://eur-lex.europa.Eu/ (2017, accessed 10 July 2018).

31. Ravikumar K, Krishnan S, Ramalingam S and Balu K. Optimization of process variables by the application of response surface methodology for dye removal using a novel adsorbent. *Dyes Pigm* 2007; 72(1): 66–74.

32. Karimi F, Rafiee S, Taheri-Garavand A and Karimi M. Optimization of an air drying process for artemisia absinthium leaves using response surface and artificial neural network models. *J Taiwan Inst Chem Eng* 2012; 43(1): 29–39.

33. Bohl T, Smallbone A, Tian G and Roskilly AP. Particulate number and nox trade-off comparisons between hvo and mineral diesel in hd applications. *Fuel* 2018; 215: 90–101.